

Experimental Study on Mechanical Behaviour of Glass Fiber Reinforced Polymer Bars under Compression

Wedeselassie Danayt Abraham ^a, Wodajo Sara Desalegn ^a, Xie Fang ^{a*}, Yang Hongmei ^a, Liang Min ^a

^a School of Civil Engineering, Shaoxing University, Shaoxing 312000, Zhejiang Province, China.

abrahamdanayt@gmail.com, fangxieusx@163.com

Abstract

The requirements for using GFRP bars are growing as several researchers have shown the functionality of bars in concrete columns. The demand to characterize the mechanical properties of GFRP bars is therefore rising, although there is no standardized test method for evaluating the compressive behavior of these bars. This experimental study presents the determination of the mechanical properties of GFRP composite bars in compression, namely the stress-strain curves, compressive strength, ultimate crushing strain, and modulus of elasticity. The compressive properties of these bars were calculated following ASTM D695-10 (Compression Test) with some modifications. A total of 27 specimens were tested for the proposed test procedure. The diameter of the GFRP tendon used in the test was 10, 12, and 14 mm, and the length to bar diameter ratio L_c/d_b (4, 8, and 16) was investigated for the compressive strength of the bars. These two parameters were used to establish the relationship between the length to diameter ratio and strength. Besides, two steel caps with a length of 50 mm each were installed to both ends of each specimen to avoid premature failure. It was observed that the test method enables to successfully evaluate the compressive characteristics of the GFRP bars. Experimental discussions were performed based on the test results from stress-strain curves, bar graphs, and scatter curves. The results indicate the increase in length to diameter ratio decrease the buckling stress and the compressive to tensile strength ratio for L_c/d_b ratio of 16 specimens in buckling failure mode. The failure mode transformed from crushing to buckling and a combination of crushing and buckling between the two different failures modes with an improvement in the L_c/d_b ratio. It shows that there was no yield section on the test specimens during the entire test loading process. The compressive GFRP bars present typical brittle failure.

Keywords: *Compressive Test, GFRP Bars, Diameter, L_c/d_b Ratio, Stress-Strain Curve, Buckling*

DOI: 10.7176/CER/13-5-04

Publication date: August 31st 2021

1. Introduction

Corrosion is possibly the biggest civil engineering problem that causes architects, governments, and contractors to spend billions of dollars on the reconstruction of steel-enhanced concrete structures. The primary aspect of using fiberglass bars as an internal reinforcement is that it allows concrete structures to achieve long service life without significant maintenance [1]. The use of Fiber Reinforced Polymers (FRP) began in the building industry in the 1970s. It was not until the 1990s, however, that non-metallic bars began replacing steel bars as internal reinforcements in concrete structures. The primary reason for this reinforcement transformation was the expensive problem of corrosion in steel-reinforced concrete structures. There has been a substantial increase in the quality and quantity of composite reinforcement around the world over the last 20 years. The advance in manufacturing technology leads to an increase in production volume, the cost of high-strength reinforcement of FRP has decreased, and has become more readily available on the market. The use of Glass Fiber Reinforced Polymer (GFRP), better known as fiberglass rebar, is a perfect way to fully eliminate the risk of corrosion in building structures. This is an alternative material used in the building industry for steel. GFRP's features vary from being corrosion-free, being lightweight, having a long product life to being stronger than steel itself [2]. Despite numerous studies on concrete members reinforced with GFRP bars, there is no standardized test method for evaluating the compressive characteristics of GFRP bars. Due to the lack of such a test procedure, there are some doubts and gaps in the compression behaviour of the GFRP bars which have led to a lack of awareness of their compressive characteristics. For example, the current American guideline for the design of fiber-reinforced polymer (FRP) bars in concrete structures [3] neglects the contribution of GFRP bars to compression and

requires the designer to replace them with concrete for the design process. Also, the Canadian Guideline for the Design and Construction of Building Structures with FRP [4] requires the use of GFRP bars in concentrically loaded columns where their contribution to the strength of the column is ignored. Despite the limitations, recent studies have shown that the neglect of the contribution of compressive GFRP bars in concrete columns is conservative [5-9]. Recent studies have also adjusted the trend of the most recent design guidelines.

In recent years, there has been a rising demand for the use of GFRP bars as longitudinal reinforcements for concrete columns. Several studies have demonstrated the efficacy of the use of GFRP bars for solid and hollow concrete columns [4, 10-15]. These studies underscored the linear elastic response to the failure of the GFRP bars as internal reinforcement in concrete columns. Some test standards [16-18] define the appropriate testing and characterization of GFRP bars to ensure the consistency and performance of the product. On the other hand, ASTM D695 [19] is generally referred to when determining the compressive properties of rigid plastics; however, the criterion does not apply to round GFRP bars. Since there is still no standard method for measuring and characterizing the compressive properties of GFRP bars due to the complex compression behavior and the various failure modes, the contribution of GFRP bars is often overlooked in the design and analysis of reinforced concrete columns. The key explanation for this is the non-homogeneity and anisotropic nature of GFRP reinforcements, where shear and transverse tensile forces have a major effect on their compressive behavior [14]. In most cases, the compressive strength of GFRP bars is stated to be a fraction of their tensile strength. There is therefore a need to establish a new method for testing and characterizing the compressive actions of GFRP bars to advance their use as longitudinal reinforcements in concrete columns.

Many studies have been performed on the characterization of GFRP bars in compression. E. Bruun (2014) [20], explores an experimental program consisting of 34 specimens of 25M GFRP bars examined under direct compression; the length of the specimens varied to determine the relationship between length and strength. Pure crushing failure within the ultimate compressive strength of 730 MPa was observed for all specimens with a nominal unbraced length of 230 mm. Longer specimens failed due to the global buckling of the bar, with the ultimate compressive strength reducing with increasing bar length. The average compressive elastic modulus was estimated to be 60 GPa.

Q.S. Khan, M.N. Sheikh, and M.N. Hadi (2015) [21] tested five GFRP and five (CFRP) bars. The GFRP bars were 80 mm long with a diameter of 15.9 mm and were tested using ASTM D695-10 [19] the standard procedure for the compressive properties of rigid plastics. The experiments included the use of parallel steel plates at the ends of the GFRP bars and the use of a displacement control method at a rate of 1.0 to 1.3 mm/min. The specimens were located directly between the steel plates to simplify ASTM D695-10 [19] by replacing the hardened end blocks with smooth and high-strength steel plates. Failure has been stated to have occurred due to the separation of the fibers that may be the result of resin failure. The modulus of elasticity and strength of the GFRP bars in tension was found to be 65 percent and 35 percent higher than their compressive counterparts, respectively.

Alajarmeh, O. S. et al. (2019) [22], has introduced a novel test method for the determination and characterization of the compressive properties of high modulus FRP bars. During the preparation of the test specimens, hollow steel caps filled with cement grout were used to contain the top and bottom ends of the GFRP bars. The effects of the bar diameter (9.5, 15.9, and 19.1 mm) and the unbraced length-to-bar diameter ratio of L_u/d_b (2, 4, 8, and 16) on the compressive strength of the bars were investigated. The findings showed that the increase in bar diameter increased the micro-fiber buckling and decreased the compressive to tensile strength ratio. Similarly, the failure mode changed from crushing to buckling with an improvement in the L_u/d_b ratio. Simplified theoretical equations have been proposed to accurately explain the compressive behavior of GFRP bars with various bar diameters and L_u/d_b ratios.

Overall, different test fixtures were used to classify GFRP bars in compression by researchers [10, 21-22]. However, different observations have been made on the compressive strength and elasticity modulus of these proposed test methods, as stated earlier. The free length to diameter ratio varied from test to test, and the failure modes were either the buckling of the bar, the buckling of the fibers after separation of the resin, or the crushing of the end. The latter may trigger observations that showed less compressive strength for GFRP bars due to buckling (high free length to diameter ratios) or due to biaxial stress (very small free length to diameter ratios). Also, for some of the proposed test methods, there was space for a final rotation that allowed the GFRP compressive coupon to experience a combination of flexural and axial loading which in turn, resulted in a lower compressive strength. The other concern will be the crushing at the end of the GFRP bars, the impact of these should be examined. Also, it should be noted that in addition to the test methods, the consistency of the FRP bar output and the evolution of the FRP bars may be important parameters in the diversity of the values recorded for

the strength and elasticity of bars at different dates.

2. Test Procedures

2.1 Proposed Test Method

Generally, this test method suggests that the GFRP bar, which is embedded in adhesive anchors and steel caps at both ends, should be checked in a mechanical test machine under monotonic compressive load up to failure while monitoring load and longitudinal strain. This project aimed to assist researchers and designers in assessing the stress-strain curve, compressive strength, crushing strain, and modulus of elasticity of the GFRP bars for the compression test. One of the characteristics of this test method is the gripping and alignment during the test specimen preparation process instead of in the test machine. The steel cap and adhesive anchors act as a gripping method by enclosing the ends of the GFRP bars to avoid premature failure and allow them to obtain their full compressive capacity. Also, the alignment can be simply done when the adhesive anchors are mounted at a level that can avoid unnecessary bending and premature failure and increase the accuracy of the test results, especially longitudinal strains. This study recommends a total of 27 specimens for each test condition to record consistent and accepted data sets. The schematic illustration of the test specimen is shown in Figure 1. Test fixture elements include plastic cover, steel cap, electrical tape (insulating tape), and adhesive anchors. The diameter of the steel cap was proposed to be considered twice the effective bar diameter, while the length recommended was the same for all specimens with various effective length to bar diameter ratios as shown in Figure 3. The steel cap must be thicker enough not to generate or distort the lateral pressure of the adhesive anchors. The GFRP bar should be 4, 8, and 16 times as long as its diameter to provide an effective length between the steel caps. For instrumentation, it is recommended that two strain gauges be mounted on two opposite sides in the center of the bar to record longitudinal strains. Strain gauges are the appropriate measuring instruments for this test configuration. The average of two strain gauges is a good alignment indicator if properly mounted. If the difference between the measured strains is not important, the mean value of the two strain gauges is assumed to be the longitudinal strain, otherwise, the current misalignment contributes to the formation of bending in bars and the test results are not accurate.

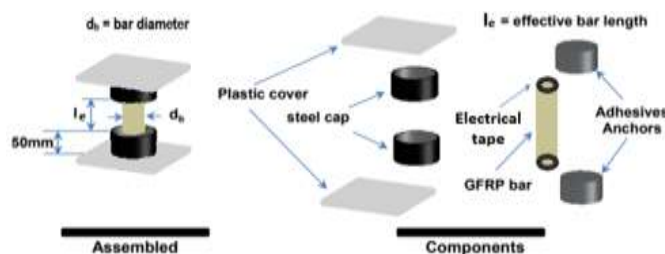


Figure 1. Proposed test fixture.

Once the preparation and instrumentation have been completed, the specimens are examined by applying a uniform and monotonous compression force. To spread the load more equally to the steel caps. It is recommended that the tests are carried out using the displacement control method at a test rate that results in the completion of the test in 30 minutes. The test results are considered appropriate if no premature failure of the caps or the effective length of the buckling is observed. In other words, tests are carried out successfully when the crushing of GFRP bars happens at the free length of the specimen.

2.1 Test Materials

2.2.1 GFRP Bars

In this study, three GFRP bars with a diameter of 10, 12, and 14 mm were considered. The bars contain glass fibers that have been impregnated with epoxy resin using a pultrusion process. The rebars are ribbed in a comparable way to the deformed steel rebars. The GFRP bars used in this test study were manufactured at the same time and produced by the same company as Shandong Stifford Industrial Co., Ltd. In this study, these bars are explicitly chosen to meet the standard specifications for structural compression members




Figure 2. Considered GFRP bars

2.2.2 Steel Cap

In this research, the test method involves the preparation of GFRP bar samples with top and bottom end caps allowing the positioning of the specimens inside the test machine and the application of concentric loads. Besides, the use of two heavy steel plates, which if present, could affect the measured bar strength, was removed. In this test approach, the top and bottom ends of the thick composite laminates were steel-capped to reduce stress concentration in the load application zones and to facilitate failure within the effective length. In the preparation of the test specimens, the diameter and thickness of the steel tubes for the end caps are based on the recommendation of ASTM D7205/D7205M-06 [23] for the tensile testing of the GFRP bars shown in Table 1.



Figure 3. Front and top view of the steel cap.

	Bar Diameter, d_b (mm)	10	12	14
	Outer Diameter, d (mm)	25	27	29
	Wall thickness, t (mm)	3	4	4
	Height, h (mm)	50	50	50

2.2.3 Adhesive

The main objective of the anchoring system was to allow the adhesive material (504 AB) to be spread inside the thick-walled steel cap to clamp the rebar into an anchor with the appropriate length for load transfer. It was used to regulate the lateral expansion of the upper and lower ends of the GFRP bars under the compression load. Due to the higher stiffness of the steel cap, the adhesive material exerts pressure on the rebar specimen, which preserves the specimen location inside the steel tube. It was used to prevent the lateral expansion of the upper and lower ends of the GFRP bars under the compression load.



Figure 4. Adhesive anchor glue.

2.3 Test Matrix and Specimen Fabrication

The GFRP bar specimens for compressive tests were developed and prepared to have various effective lengths. Three L_e/d_b ratios of (4, 8, and 16) were considered in this test, where d_b is the bar diameter and L_e (effective bar length) is the clear length between two steel caps as shown in Figure 4. Three number (N) replicates (A, B, and C) were prepared for each L_e/d_b ratio. Therefore, in this study, nine specimens were prepared for each bar diameter of 10, 12, and 14mm with a total of 27 specimens of GFRP bars. Table 2 provides the effective length (L_e) and the total length (L_T) in mm of the test specimens. Figure 5 shows the schematic diagram of a test specimen. The samples were named by “G” as in GFRP followed by the L_e/d_b ratio, in the middle the bar diameter was designated and then the sample number. For example, G 4d-10-A is a GFRP bar of (10 mm diameter) with L_e/d_b ratio of 4 and a test piece of label A.

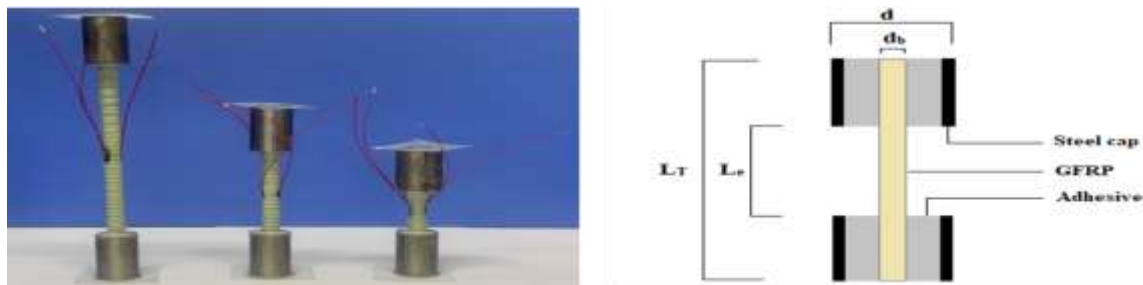


Figure 5. Schematic Diagram of the Specimen

Table 2. Sample design matrix

d_b (mm)	$4d_b$		$8d_b$		$16d_b$	
	L_e	L_T	L_e	L_T	L_e	L_T
10	40	140	80	180	160	260
12	48	148	96	196	192	292
14	56	156	112	212	224	324

The same fabrication and testing procedures were used for each specimen. The only variable parameter in this study was the effective length of the specimen. All the specimens were cut and manufactured in the same batch to ensure uniform material properties.

GFRP bars were prepared following these steps before the fabrication of specimens:

1. Individual specimen lengths were measured and marked.
2. Specimens were cut to size using a fiber saw blade.
3. Ends were made perpendicular with a rotating lathe.
4. For the placement of the strain gauge, the surface of the GFRP bar at mid-height was shallowly machined, in other words, the surface was flattened using a milling machine on the opposite sides of the bar (which gives a depth of around 1 to 2 mm to the machined area).

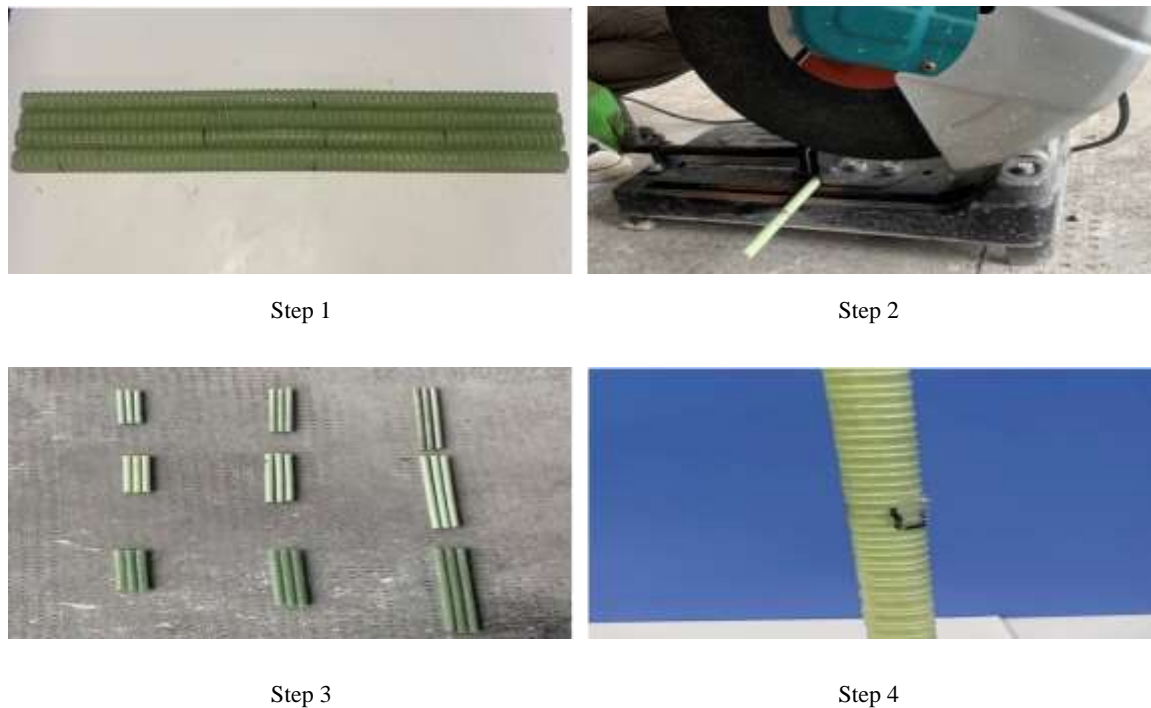


Figure 6. Preparation steps of GFRP tendon before fabrication

The preparation of the specimens is directly related to the consistency of the test results, as the alignment and capping criteria must be achieved during the preparation process. Figure 7 presents the fabrication process for compressive GFRP bar specimens.

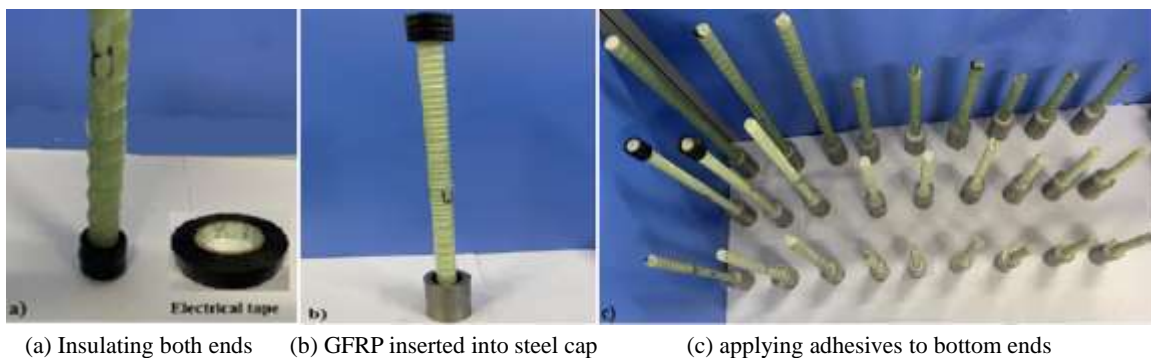


Figure 7. Fabrication of GFRP Specimen

First, on both ends of the GFRP bar, the electrical tape (insulating tape) was used to maintain the position of the bar at the center when inserted into the steel tube. The adhesive anchor was then used to fill the gap between the steel tubes and the bars. When passing the top of the steel cap, the excess adhesive was removed. According to the specifications provided by the manufacturers of adhesive anchors, the total setting time for both specimen anchors were 72 hours in typical indoor laboratory conditions. Following the specification, the first anchor was turned upside down after 72 hours and the same process was repeated for the second anchor of the bar to have both steel caps appropriately mounted at the ends of the GFRP bar shown in Figure 8.

2.3.1 Test equipment and loading scheme

It is noted that each specimen is prepared according to the test preparation referenced in the proposed test method section. The schematic test setup and the instrumentation are shown in Figure 9. Before starting the test, two strain gauges (namely SG1 and SG2) with a length of 3 mm on the opposite sides of the GFRP bar tested

were mounted on the mid-height of the machined area to record the stress-strain behavior shown in Figure 8.



Figure 8. Specimens for testing

All samples were under concentric compressive load until failure using the test machine (Shaoxing university 600 kN hydraulic servo universal) as shown in Figure 9. The applied load and strain data were reported using the TST3827E dynamic and static strain gauge data logger. It should be noted that the upper loading steel platen allowed the sample to have some rotation suggesting a pinned-end attachment, which is the ideal behavior for reinforcing bars under compression, as indicated by other researchers. The adopted displacement rate was 5 mm/min for failure to occur within 1–30 min, except for premature failure.

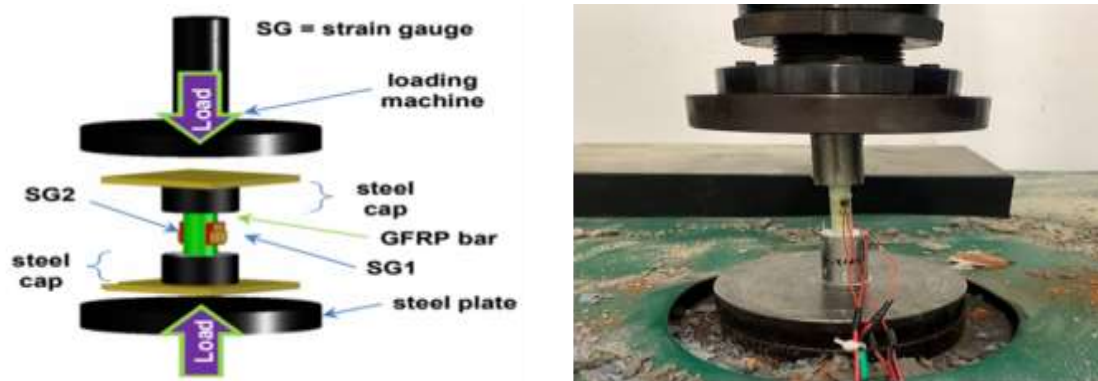


Figure 9. Set-up of Compression test

2.4 Designed tensile bars

In this study, tension testing was designed to investigate the action of the compressive to tensile strength and the modulus ratio. All GFRP bars were produced at the same time and arrived from the same company for both tension and compression tests. The total length of the test piece was 1000 mm, the effective length of the middle segment was 400 mm, and the two ends were anchored by a smooth steel pipe with a length of 300 mm. In this test, the tensile properties of the GFRP bars with three different diameters were evaluated and the effect of the diameter and length of the test bars on the tensile properties of the GFRP bars was analyzed. It is worth noting that the CSA S807-10 [16] recommends only 5 duplications for the tensile test of GFRP bars. To ensure the reliability of the test results, a total of 3 groups of 5 test pieces per group with a total of 15 test pieces were prepared. The mechanical properties of GFRP tensile bars are shown in Table 3. The standard deviation of the results is given in the parenthesis.

Table 3. Tensile properties of the GFRP bars.

Sample diameter (mm)	Ultimate tensile strength, f_{fu} (MPa)	Tensile modulus of elasticity, E_{fu} (GPa)	Ultimate tensile strain, ϵ_u (%)
10	1312.6 (177.63)	60.836 (0.526)	0.0214 (0.003)
12	1289.6 (65.87)	53.832 (1.23)	0.983 (1.31)
14	1290.4 (26.34)	52.812 (0.36)	2.44 (0.052)

3. Test Results and Analysis

3.1 Failure modes

Three modes of failure such as crushing, buckling, and shearing along with cracking and splitting thread in few specimens was observed in the GFRP bars tested in compression, which were highly influenced by the L_e/d_b ratio for every bar diameter. More details of the observed mode of failure are described below:

3.1.1 Crushing failure

Crushing failure mode was observed for bars with L_e/d_b ratio = 4, regardless of bar diameters. It was also followed by cracks as shown on the surface of the bar in Figure 10. In this mode of failure, the shear effect was not observed. Some bars suffered from localized crushing either at the top or bottom end heads. This localized crushing is caused by the damage in the matrix due to the high-stress concentration at the top and bottom ends of the bars. This phenomenon can be related to the weak strength of the GFRP bars in the transverse direction where the lateral expansion resistance is provided only by the matrix.



Figure 10. Mode of failure for bars with 4 L_e/d_b ratios for GFRP bars.

3.1.2 Combination of Crushing and Buckling

The second mode of failure was a combination of crushing and buckling of GFRP bars with surface cracks shown in Figure 11. This mode of failure was observed for all bars with $L_e/d_b = 8$. Besides, it shows higher E_{fc} and E_{fu} values for 10 mm and 14 mm tested GFRP specimens. It was also observed that the severity of the damage increased due to the larger bar diameters.

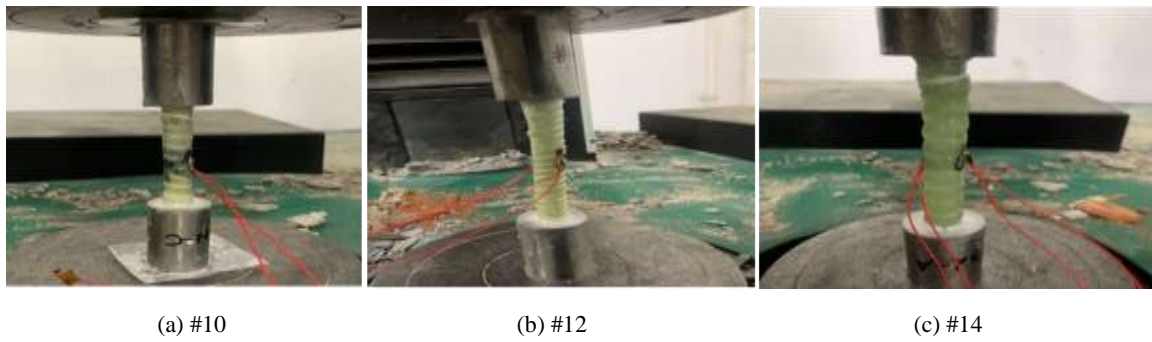


Figure 11. Mode of failure for bars with 8 L_e/d_b ratios for GFRP bars.

3.1.3 Buckling Failure

Buckling failure of the whole effective length was observed for all samples with L_e/d_b ratio = 16 regardless of the bar diameter shown in Figure 12. After the applied load was removed, the failed samples returned to their original straightened positions but with the longitudinal cracks occurring on the outer surface. As shown in Figure 12 (d) eventually all the specimens failed by shear at about 45° axes on the weakest spot of the rib length. The longitudinal cracks were caused between the fibers and the matrix due to the huge curvature under load.

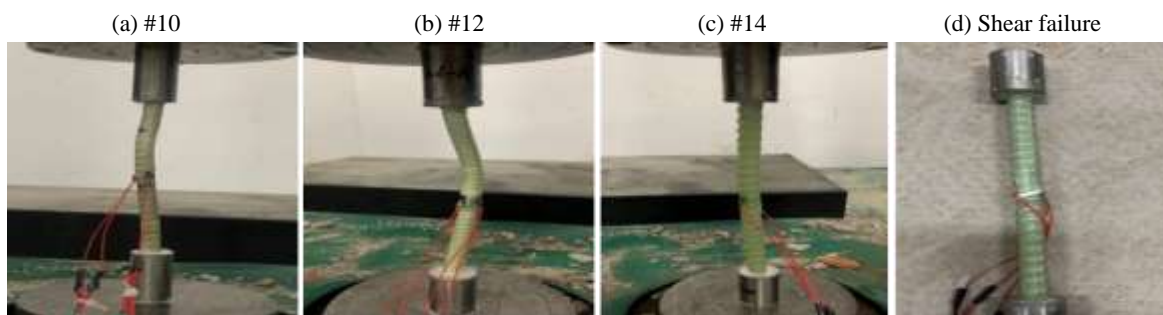


Figure 12. Mode of failure for bars with 16 L_e/d_b ratios for GFRP bars.

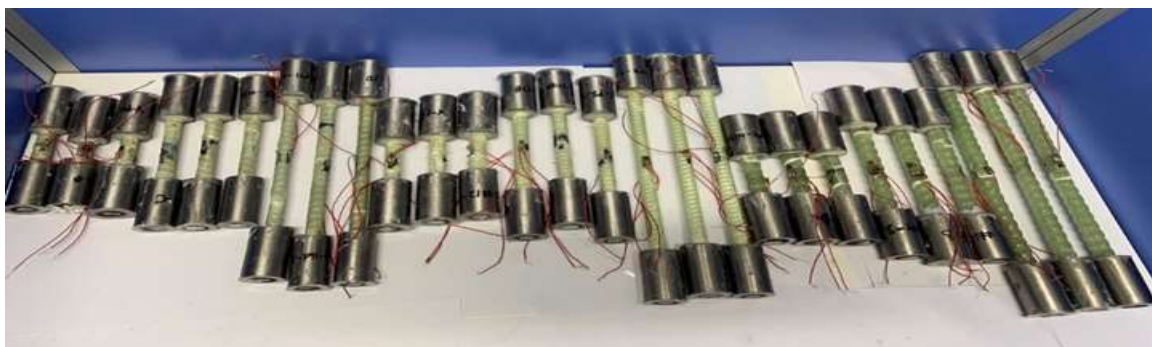
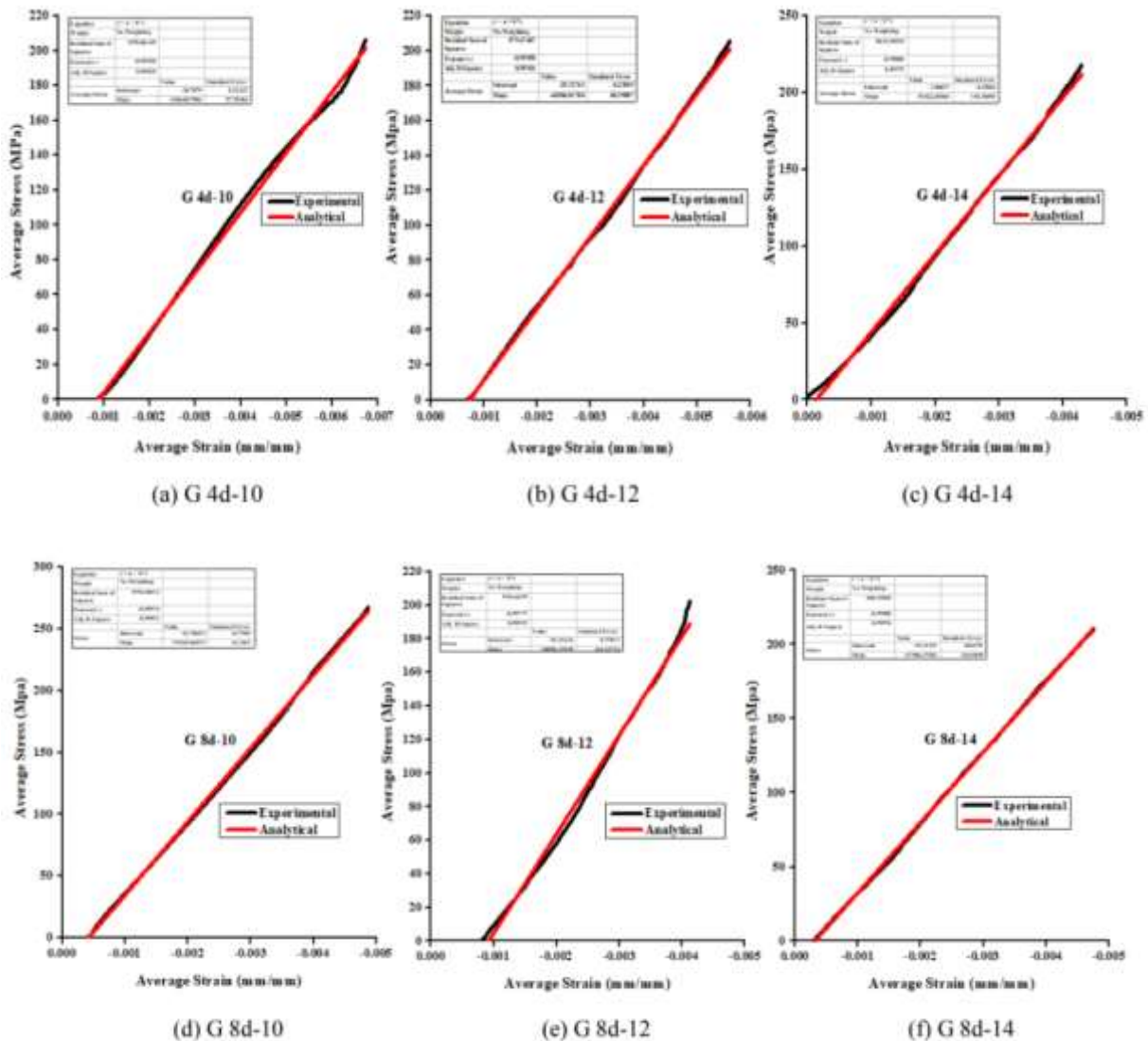


Figure 13. Tested GFRP bars with various L_e/d_b .

3.2 Determination of Compressive Characteristics

3.2.1 Stress-Strain Behavior

This section presents the typical stress-strain behavior of GFRP bars with different L_e/d_b ratios. A linear elastic stress-strain behavior was found in GFRP bars with L_e/d_b ratio = 4 regardless of the bar diameter shown in Figure 14 (a, b, and c). Moreover, an almost similar strain reading was measured by the strain gauges attached on both sides of the bars indicating that the load was applied concentrically and there was no bar buckling until failure. This stress-strain stability was observed up to the failure of the bars that exhibited localized crushing shown in Figure 10. On the other hand, GFRP bars with L_e/d_b ratio = 8 shown in Figure 14 (d, e, and f) exhibited linear elastic stress and strain behavior but not elastic as L_e/d_b ratio = 4. A different stress-strain behavior was exhibited by the GFRP bars with $L_e/d_b = 16$ shown in Figure 14 (from g to o). For both attached strain gauges, stress-strain behavior was linear up to a strain of around $-5000\mu\epsilon$, this is then followed by a nonlinear stress-strain behavior, where one gauge shows significantly increasing compressive strain with a minor increase in the stress while the other gauge starts to shift from compressive to tensile strain. The compressive strength of the buckling failure decreased with the increase in bar diameter from 196.40 MPa to 147.9 MPa for bar diameter 10 mm and 12 mm, respectively. Meanwhile, it attained a maximum f_{fc} value of 215.22 MPa for a bar diameter of 14 mm. The maximum measured axial strain in compression (ϵ_c) is 0.0066 for the tested GFRP bars. As shown on the stress-strain curve below analytical and experimental results have been analyzed on the graph using the average test results values with various L_e/d_b ratio.



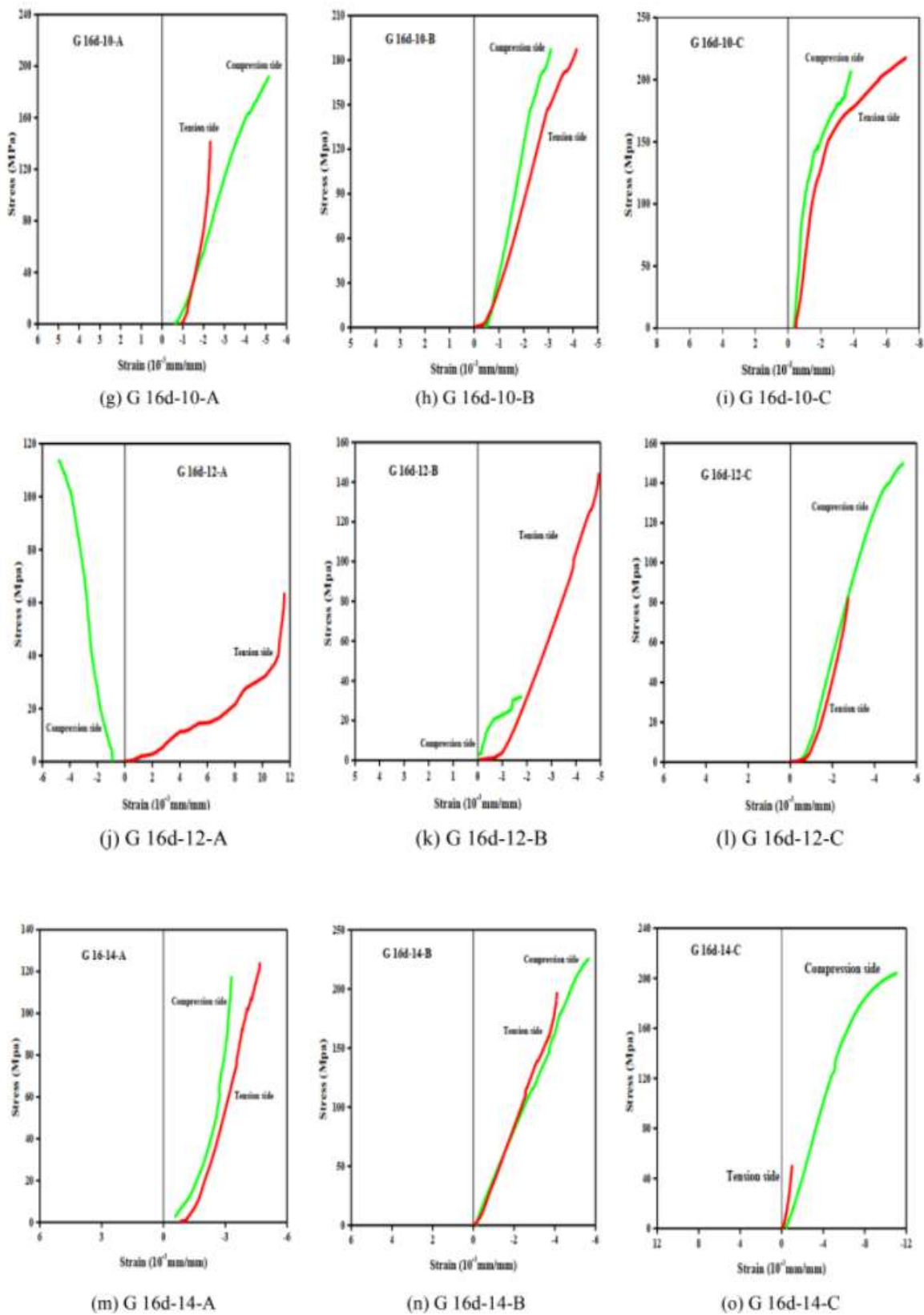


Figure 14. Typical stress-strain behavior of the tested GFRP bars with different $L_c=d_b$ ratios.

3.2.2 Compressive Strength (f_{fc})

The f_{fc} was calculated by dividing the maximum load (F_c) with the cross-sectional area of the GFRP bars shown in equation (1). However, there was no difference between the specimens with different modes of failure in terms of determining their compressive strength and modulus of elasticity.

$$f_{fc} = \frac{F_c}{A} = \frac{4F_c}{\pi d^2} \quad (1)$$

Where f_{fc} is compressive strength in MPa; F_c is compressive ultimate load value of the test piece in N; d is the diameter of the test piece in mm.

Table 4 summarizes the test results of the compressive strength (f_{fc}) for all tested GFRP bars. The test results generally show higher f_{fc} values for bar diameter 10 mm compared to 12 and 14 mm. The maximum average f_{fc} value recorded for bar diameter 10 mm is 323.36 MPa, while it is 276 MPa and 280 MPa for 12 and 14 mm bar diameters, respectively. It can be noticed in Table 4 that f_{fc} values for bar diameter 10 and 14 mm are higher with L_e/d_b ratio = 8, while it is significantly lower than that for bar diameter 14 mm. Furthermore, a significant drop in f_{fc} values was measured for all bar diameters at L_e/d_b ratio = 16. On the other hand, the average f_{fc} values for bar diameter 10 and 14 mm increase as the L_e/d_b ratio increases from 4 to 8. On the contrary, a consistent and convergent f_{fc} average values were observed for bar diameter 12 and 14 mm. As shown on Table 4, the standard deviation (SD) and coefficient of variation values (CoV) are not consistent when compared with each other.

Table 4. Compressive Strength (f_{fc}) (MPa) of the tested GFRP bars with various L_e/d_b .

Sample no.	10 mm bar L_e/d_b ratio			12 mm bar L_e/d_b ratio			14 mm bar L_e/d_b ratio		
	4	8	16	4	8	16	4	8	16
A	200.53	341.33	192.38	274.90	219.71	118.45	237.07	263.59	215.92
B	-	307.38	186.81	-	234.06	173.88	249.62	296.40	225.66
C	205.98	-	210.02	278.2	220.48	149.85	-	-	204.07
Average	203.26	323.36	196.40	276.55	224.75	147.39	243.35	280	215.22
SD	3.85	24	12.12	2.33	8.07	27.79	8.87	23.20	10.81
CoV (%)	1.894	7.4	6.17	0.843	3.59	18.86	3.64	8.28	5.02
$(f_{fc}/f_{fu}) * 100$	15.49	24.71	14.96	21.44	17.42	11.43	18.85	21.70	16.60

3.2.3 The Comprehensive Modulus of Elasticity (E_{fc})

The compressive modulus of elasticity (E_{fc}) was calculated and reported in Table 5. Similar to the approach suggested by CSA S806 [16] and ASTM D7205/D7205M [23] to determine the tensile modulus of elasticity of GFRP bars, the E_{fc} values of GFRP bars were measured from the slope between 0.001 and 0.003 mm/mm. The average result, standard deviation (SD), and coefficient of variation (CoV) of 3 identical specimens in each L_e/d_b ratio for different bar diameters were obtained. As reported in Table 5, very close E_{fc} and E_{fu} values were obtained for a bar diameter of 12 and 14 mm. E_{fu} values for 10, 12, and 14 mm are higher than E_{fc} values for all diameters by 13.32%, 14.36%, and 14.6%, respectively. Moreover, L_e/d_b ratio = 8 for all bars diameter showed a higher E_{fc} , and also higher standard deviation (SD), and coefficient of variation (CoV) of the test results compared to L_e/d_b ratio = 4 and 16 GFRP bars.

Table 5. Compressive elastic modulus (E_{fc}) (GPa) of the tested GFRP bars with various L_e/d_b ratios.

Sample no.	10 mm bar L_e/d_b ratio			12 mm bar L_e/d_b ratio			14 mm bar L_e/d_b ratio		
	4	8	16	4	8	16	4	8	16
A	-43.53	-46.70	-45.9	42.10	-75.65	-31.25	-45.50	-43.55	-36.43
B	-	-76.55	-76.74	-	-47.47	-31	-52.32	-56.1	-44.5
C	-36.23	-	-47.16	-43.37	-59.81	-41.5	-	-	-28.75
Average	-40	-61.71	-56.60	-42.73	-60.98	-34.57	-48.91	-49.83	-36.54
Average all	-52.73			-46.1			-45.1		
SD	3.652	14.84	14.25	0.632	11.54	4.9	3.4	6.3	6.41
CoV (%)	-6.93	-28.15	-27.03	-1.37	-25.02	-10.61	-7.56	-13.92	-14.23
$(E_{fc}/E_{fu}) * 100$	-65.55	-101.4	-93.04	-79.38	-113.3	-64.22	-92.62	-94.34	-69.2

3.2.4 The Ultimate Comprehensive strain (ϵ_c)

The ultimate crushing strains were derived by dividing the compressive strength by the compressive modulus of elasticity, as presented in equation 2.

$$\epsilon_c = \frac{F_c}{E_{fc}A} \quad (2)$$

Where ϵ_c is the compressive ultimate strain in mm/mm; F_c is the compressive ultimate load value of the test piece in N; E_{fc} is the compressive elastic modulus in GPA; A is the cross-sectional of the test piece in mm².

Table 6. Ultimate compressive strain (ϵ_c) (mm/mm) of the tested GFRP bars with various L_e/d_b ratios.

Sample no.	10 mm bar L_e/d_b ratio			12 mm bar L_e/d_b ratio			14 mm bar L_e/d_b ratio		
	4	8	16	4	8	16	4	8	16
A	-0.0047	-0.0073	-0.0042	-0.0067	-0.003	-0.0038	-0.0053	-0.0061	-0.006
B	-	-0.0041	-0.0025	-	-0.005	-0.0057	-0.0048	-0.0053	-0.0051
C	-0.0057	-	-0.0045	-0.0065	-0.004	-0.0037	-	-	-0.0071
Average	-0.0052	-0.0057	-0.0037	-0.0066	0.004	-0.0044	-0.0051	-0.0057	-0.0061

4. The factors of Compressive Characteristics

4.1 The influence of bar diameter

The bar diameter does not affect the failure mode of the GFRP bars with the same L_e/d_b ratio. For bars with L_e/d_b ratio = 4, all the bars failed by crushing while the bars with L_e/d_b ratio = 16 failed by buckling, and those with L_e/d_b ratio = 8 failed by a combination of crushing and buckling. As often observed in GFRP bars under stress, there is a non-uniform stress distribution across the cross-section of the bars, wherein higher stress is experienced by the outer fibres compared to the fibers at the center of the bar. The figures below show the comparison of GFRP specimens with various L_e/d_b ratios.

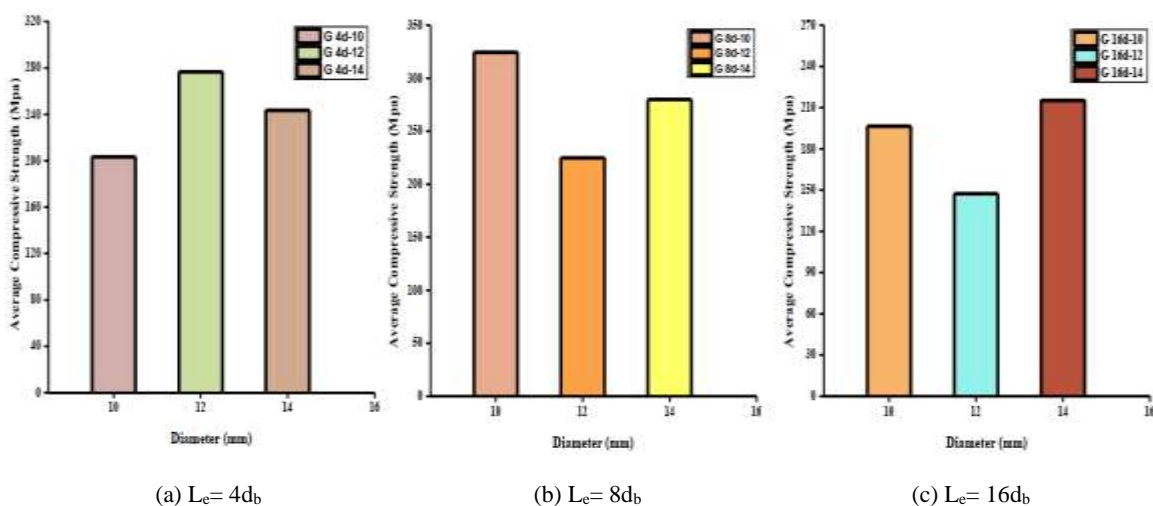


Figure 15. Average Comprehensive Strength versus diameter

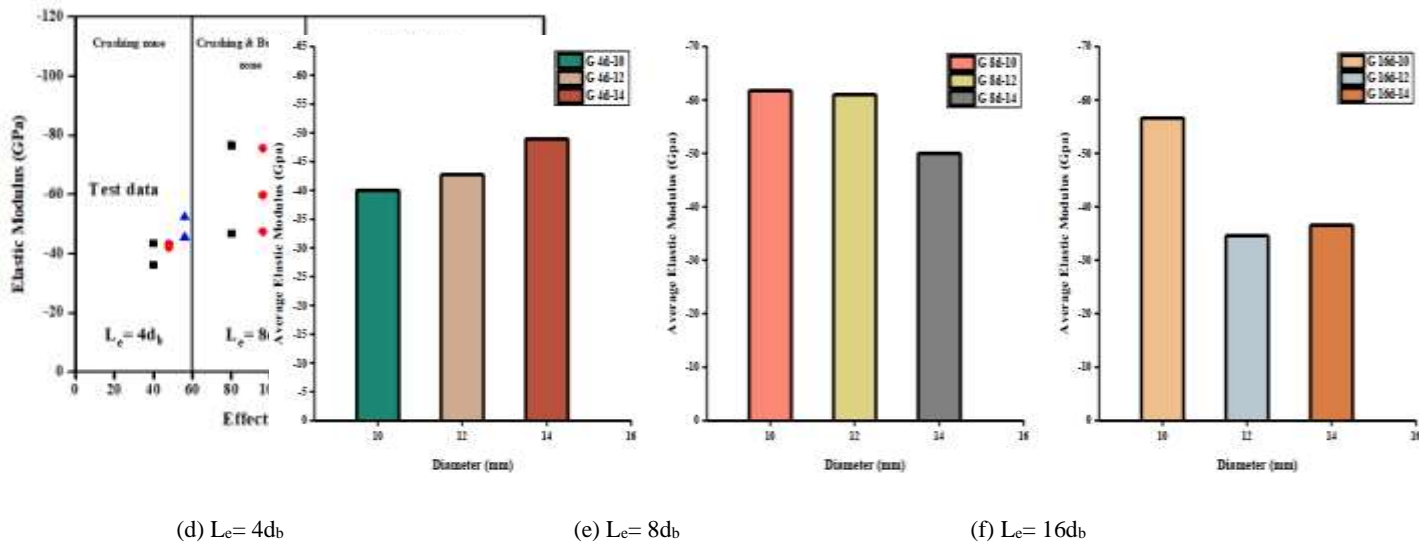


Figure 16. Average Modulus of Elasticity versus Diameter.

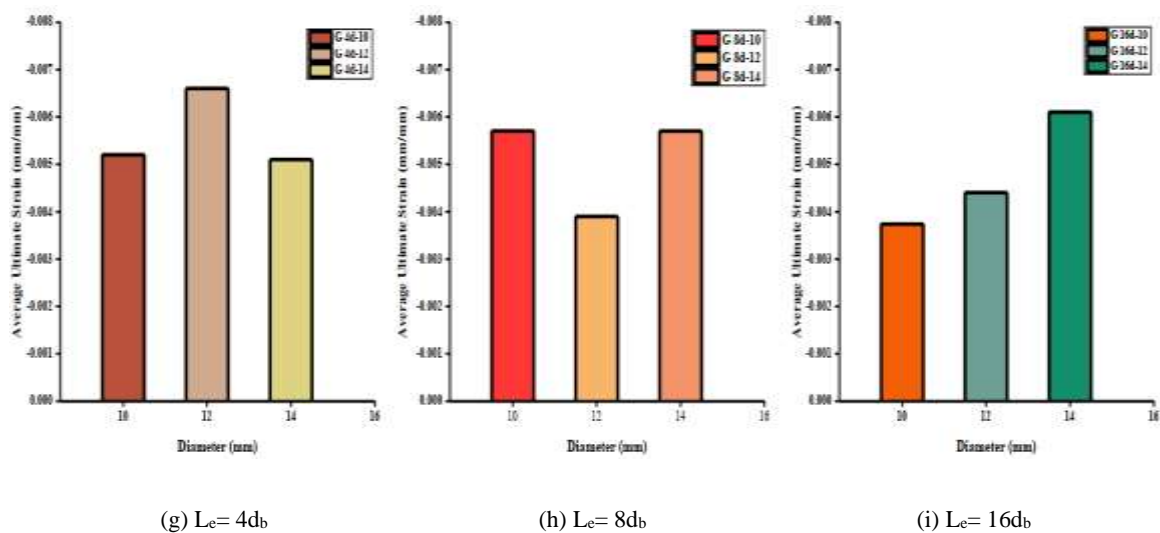


Figure 17. Average Ultimate strain versus Diameter.

4.2 Influence of slenderness ratio

The following Figures 18 and 19 illustrate the relationship between Elastic modulus/ Average elastic modulus and the effective length of the GFRP bars. Maximum elastic modulus value (E_{fc}) of bar diameter 10 mm is attained for L_e/d_b ratio = 8. When compared E_{fc} value increases from L_e/d_b ratio = 4 to 8 and decreases from L_e/d_b ratio = 8 to 16. So GFRP specimens have higher values of L_e/d_b ratio = 8 for both elastic modulus versus effective length graph and compressive to tensile strength ratio versus L_e/d_b ratio graph shown in Figure 20.

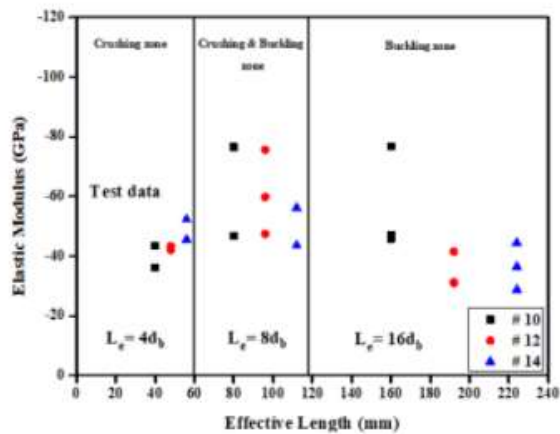


Figure 18. Elastic modulus versus effective length all specimens.

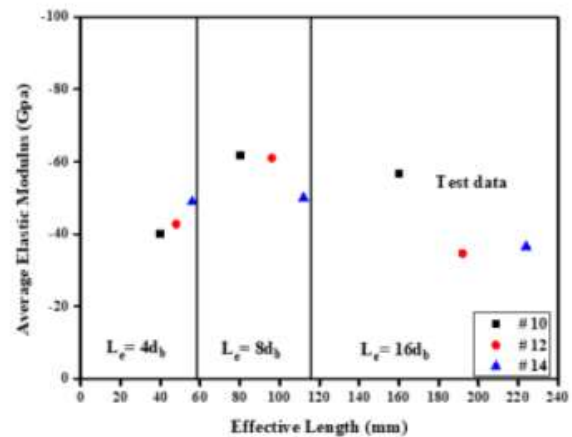


Figure 19. Average Elastic modulus versus for Effective length for all specimens.

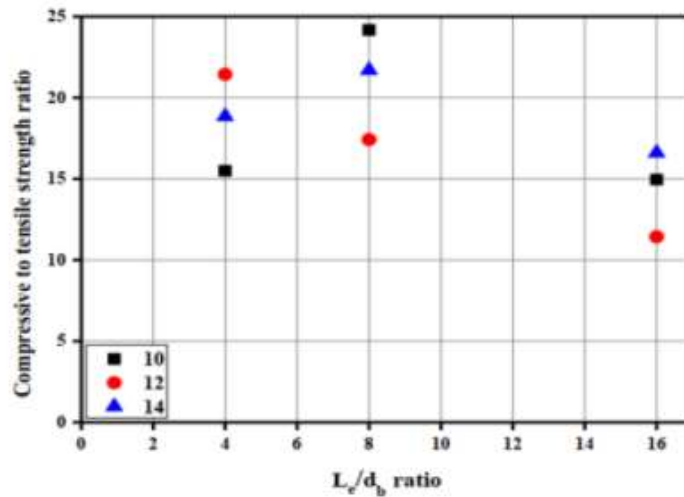


Figure 20. Compressive strength to Tensile strength ratio vs L_e/d_b ratio of the tested GFRP bars.

4.3 The mechanics of buckling failure

The Euler formula, shown in Equation (3) is the most common equation used for estimating the elastic buckling load of homogeneous material. In this relation, E_{fc} is the compressive modulus of elasticity of the material and is the slender ($\frac{k l_e}{r}$) ratio. This equation was modified to account for the non-homogenous nature of the GFRP bars. It should be mentioned that GFRP bars with $L_e/d_b = 16$ will have ratio of 32. The $\frac{f_{bc}}{f_{bc-b}}$ s showed a high variation between the experimental (f_{bc-b}) and theoretical (F_{b-eu}) buckling stresses, as shown in Figure 21. Note that the k factor is assumed to be 1.0. This assumption is supported by the ability of the upper load plate to allow some rotation in the samples during testing.

$$F_{b-eu} = \frac{\Pi^2 E_{fc}}{\left(k \frac{l_e}{r}\right)^2} \quad (3)$$

Where, k is column effective length factor, $k=1$; f_{bc-b} is experimental buckling stress in MPa; F_{b-eu} is theoretical buckling stress in MPa; r is the radius of the bar, mm.

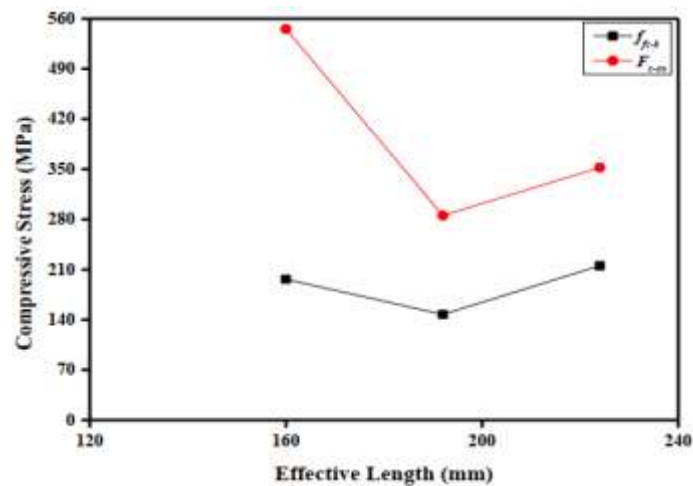


Figure 21. Comparison between Experimental and Theoretical Buckling Stress Results.

The prediction showed a great agreement between experimental (f_{fc-b}) and theoretical (F_{b-eu}) buckling stresses as presented by a red circular data point indicating that the modified Euler equation can provide an improved and reliable estimation for the buckling stress of GFRP bars.

5. Reliability of the Compressive test Method for GFRP bars

The consistency of the compressive test method was tested by evaluating the test results and contrasting the test results with those of previous studies using different test methods. The provision of steel caps filled with adhesive anchors in the top and bottom portions of the GFRP bars permitted the specimen to be positioned longitudinally upright in the equipment and facilitated the application of concentric compressive loads. There were no signs of eccentricity caused bending moment effects suggesting the feasibility of the fabrication process except for the improper fabrication of specimens. This can be shown by almost similar measurement strain readings on gauges attached to two sides of the test specimens in the linear elastic region of the stress-strain curve. Except for a misaligned single specimen with a bar diameter of 10 mm for L_e/d_b ratio = 4, no premature failure was found in the specimens tested due to high-stress levels at the top and bottom of the bars.

This result suggests that the compressive strength obtained from the crushing and buckling failure modes is substantially affected by the testing procedure. Using this test method, any premature and undesirable failure due to the impact of the test setup can be avoided to obtain test results that accurately and reliably characterize the compressive behavior and the GFRP bar strength capability. Based on the test results and study using bar graphs and scatter graphs, it was found that the bar diameter of 10 mm shows the most representative value for both the compressive strength and the tensile strength of the GFRP bars. Moreover, the most representative value for the compressive strength of the tested GFRP bar specimens is the one caused by the use of the L_e/d_b ratio = 8. Therefore, this L_e/d_b ratio is suggested for evaluating GFRP compression bars to obtain clear and accurate test results. Consequently, these observations demonstrate the good reliability of the test results using the proposed test methodology for the determination of the compressive actions of GFRP bars with different bar diameters and L_e/d_b ratios.

6. Conclusions

This study examines the effect of bar diameter and the effective length to bar diameter ratio (L_e/d_b) on the compressive behavior of GFRP bars. It is dedicated to the determination of the compressive stress-strain curve, compressive strength, the ultimate strain, and compressive modulus of elasticity of the GFRP bars by proposing a unique testing procedure. A total of 27 compressive GFRP bar specimens were tested, discussion and analysis were provided to predict the compressive strength of the GFRP bars at different L_e/d_b ratios.

Based on the results and observations, the following conclusions can be drawn:

- The proposed test method was successfully implemented to obtain the stress-strain curve, compressive

strength, ultimate crushing strain, and modulus of elasticity of the GFRP bars.

- The experimental method of testing GFRP bars under compression provided reliable and consistent compressive strength for the tested GFRP bars specimens. This method allowed the longitudinally upright positioning of specimens and the concentric application of compressive loads without causing premature failure in the bars examined.
- GFRP bars for L_e/d_b ratio = 8 gave the most representative value for both compressive strength and modulus of elasticity of the tested specimens. It is recommended for testing GFRP bars in compression. The failure behavior of GFRP bars with this L_e/d_b ratio represents closely the failure in compression of the longitudinal bars in concrete columns.
- There was a statistically significant difference between the measured compressive strength groups of GFRP bars with differing bar diameters. For GFRP bars with L_e/d_b greater than 4, the average compressive strength of the bar diameter of 10 mm is significantly higher than the bar diameters of 12 and 14 mm. This also shows a higher compressive elastic modulus of 10 mm bar than the 12 and 14 mm GFRP bars.
- The slenderness ratio (L_e/d_b ratio) greatly affected the failure behavior and load capability of the GFRP bars in compression but did not significantly affect the compressive modulus of elasticity. In general, the compressive strength of GFRP bars is significantly higher for bars with a L_e/d_b ratio of 4 to 8 than for bars with a L_e/d_b ratio of 16. Whereas for GFRP bars with L_e/d_b ratio = 8, the standard deviation and the coefficient of variance of bar diameters 10 and 14 mm of the test results show a higher compressive strength.
- Also, a revised Euler equation, solving for the effective length to bar diameter ratio and the non-homogenous properties of slender GFRP bars, was proposed to predict buckling strength.

Declaration

This thesis is a presentation of our original research work. Wherever contributions of others are involved, every effort is made to indicate this clearly, with due reference to the literature, and acknowledgment of collaborative research and discussions. This research was funded by an international program (USX-UPC-2021330001000082), which was supported by Zhejiang Qinye Construction Industry Group Co., Ltd., Zhejiang Province 312000, and a collective enterprise science and technology project (SX-JT-KJ-2018-03), which was supported by Zhejiang Electric Company of State Grid.

References

- [1] Manalo, A., Benmokrane, B., Park, K.-T., & Lutze, D. J. C. A. (2014). Recent developments on FRP Bars as internal reinforcement in concrete structures. 40(2), 46-56.
- [2] Mazaheripour, H., Barros, J. A., Sena-Cruz, J., Pepe, M., & Martinelli, E. J. C. S. (2013). Experimental Study on bond performance of GFRP bars in self-compacting steel fiber reinforced concrete. 95, 202-212.
- [3] Goldston, M. W. (2016). Behaviour of concrete beams reinforced with GFRP bars under static & impact Loading. [6] Nanni, A. (1999). 1 Composites: Coming on Strong Concrete Construction. 44(1), 120-124.
- [4] Maranan, G. B., Manalo, A. C., Benmokrane, B., Karunasena, W., & Mendis, P. (2016). Behavior of Concentrically loaded geopolymer-concrete circular columns reinforced longitudinally and transversely with GFRP bars. *Engineering Structures*, 117, 422-436.
- [5] Fillmore, B., & Sadeghian, P. (2018). Contribution of longitudinal glass fiber-reinforced polymer bars in Concrete cylinders under axial compression. *Canadian Journal of Civil Engineering*, 45(6), 458-468.
- [6] Guérin, M., Mohamed, H. M., Benmokrane, B., Shield, C. K., & Nanni, A. (2018). Effect of glass Fiber-reinforced polymer reinforcement ratio on axial-flexural strength of reinforced concrete columns. *ACI Structural Journal*, 115(4), 1049-3.
- [7] Hales, T. A., Pantelides, C. P., & Reaveley, L. D. (2016). Experimental evaluation of slender high-strength concrete columns with GFRP and hybrid reinforcement. *Journal of Composites for Construction*, 20(6), 04016050.
- [8] Mohamed, H. M., Afifi, M. Z., & Benmokrane, B. (2014). Performance evaluation of concrete columns Reinforced longitudinally with FRP bars and confined with FRP hoops and spirals under axial load. *Journal of Bridge Engineering*, 19(7), 04014020.

- [9] Tobbi, H., Farghaly, A. S., & Benmokrane, B. (2012). Concrete Columns Reinforced Longitudinally and Transversally with Glass Fiber-Reinforced Polymer Bars. *ACI Structural Journal*, 109(4).
- [10] Khorramian, K., & Sadeghian, P. (2017). Experimental and analytical behavior of short concrete Columns reinforced with GFRP bars under eccentric loading. *Engineering structures*, 151, 761-773.
- [11] Bakis, C.E., Bank, L.C., Brown, V., Cosenza, E., Davalos, J.F., Lesko, J.J., Machida, A., Rizkalla, S.H. and Triantafillou, T.C. (2002). Fiber-reinforced polymer composites for construction—State-of-the-art review. *Journal of composites for construction*, 6(2), 73-87.
- [12] Canadian Standards Association. (2012). *Design and Construction of Building Structures with Fiber Reinforced Polymers (CAN/CSA S806-12)*. Rexdale, ON, Canada.
- [13] Deitz, D., Harik, I., & Gesund, H. (2000). *GFRP Reinforced Concrete Bridges (No. KTC-00-9)*.
- [14] Tennyson, R. C., Mufti, A. A., Rizkalla, S., Tadros, G., & Benmokrane, B. (2001). Structural Health Monitoring of innovative bridges in Canada with fibre optic sensors. *Smart Materials and Structures*, 10(3), 560.
- [15] AlAjarmeh, O. S., Manalo, A. C., Benmokrane, B., Karunasena, W., & Mendis, P. (2019). Axial performance of hollow concrete columns reinforced with GFRP composite bars with different reinforcement ratios. *Composite Structures*, 213, 153-164.
- [16] S807-10, C.C., (2010), *Specifications, for fibre-reinforced polymers*. Rexdale Ontario, Canada.
- [17] ASTM D7957M-17. (2017). *Standard specification for solid round glass fiber reinforced polymer bars for concrete reinforcement*. West Conshohocken, PA: ASTM.
- [18] *Standardization: 2015: Fiber-Reinforced Polymer (FRP) Reinforcement of Concrete: Test Methods: Part 1: FRP Bars and Grids*. 2015, ISO Geneva.
- [19] ASTM D695-10. (2010). *Standard Test Method for Compressive Properties of Rigid Plastics*; ASTM: West Conshohocken, PA, USA.
- [20] Bruun, E. (2014). GFRP bars in structural design: determining the compressive strength versus unbraced length interaction curve. *Journal of Student Science and Technology*, 7(1).
- [21] Khan, Q. S., Sheikh, M. N., & Hadi, M. N. (2015). Tension and compression testing of fibre reinforced polymer (FRP) bars.
- [22] AlAjarmeh, O. S., Manalo, A. C., Benmokrane, B., Vijay, P. V., Ferdous, W., & Mendis, P. (2019). Novel testing and characterization of GFRP bars in compression. *Construction and Building Materials*, 225, 1112-1126.
- [23] ASTM D7205/D7205M, A. (2006). "Standard Test Method for Tensile Properties of Fiber Reinforced Polymer Matrix Composite Bars." ASTM International (ASTM).